

INCLUSIVE η PRODUCTION AT HIGH p_T AT THE ISR

C. Kourkouvelis and L.K. Resvanis

University of Athens, Athens, Greece

T.A. Filippas and E. Fokitis

National Technical University, Athens, Greece

A.M. Cnops, S. Iwata¹⁾, R.B. Palmer, D.C. Rahm,

P. Rehak and I. Stumer

Brookhaven National Laboratory²⁾, Upton, NY, USA

C.W. Fabjan, T. Fields³⁾, D. Lissauer⁴⁾, I. Mannelli⁵⁾, P. Mouzourakis,

A. Nappi⁵⁾ and W.J. Willis

CERN, Geneva, Switzerland

and

M. Goldberg

Syracuse University⁶⁾, Syracuse, NY, USA

ABSTRACT

The inclusive η production cross-section at the CERN ISR has been measured for p_T values of up to 11 GeV/c. We find that the η/π^0 cross-section ratio has an average value of 0.55 ± 0.07 and varies little with p_T .

(Submitted to Phys. Letters B)

-
- 1) Permanent address: Nagoya University, Nagoya, Japan.
 - 2) Research under the auspices of U.S.D.O.E.
 - 3) Permanent address: Argonne National Laboratory, Argonne, Ill., USA.
 - 4) Permanent address: Tel-Aviv University, Israel.
 - 5) On leave of absence from the University of Pisa and INFN, Sezione di Pisa, Italy.
 - 6) Work supported by the US National Science Foundation.

INTRODUCTION

Using a detector system [1] that offers both high spatial resolution and large solid angle, we have measured the inclusive η production cross-section for values of $3 < p_T < 11$ GeV/c in pp collisions at the ISR. The measurements were taken at the three c.m. energies $\sqrt{s} = 31, 53, \text{ and } 62$ GeV. Two different geometrical arrangements of the apparatus [2] were used.

EXPERIMENTAL APPARATUS

Inclusive η production was measured by detecting the two resolved decay photons from the decay mode $\eta \rightarrow 2\gamma$ with a detector system [1] based on liquid-argon - Pb-plate calorimeters of high spatial resolution and large solid-angle acceptance. The two different geometrical arrangements of the detector are described in detail elsewhere [2,3] and are shown in Figs. 1a and b.

The first arrangement, "retracted geometry", consisted of two calorimeters placed at a distance of 1.6 m from the interaction point, each calorimeter covering 70° to 110° in polar angle and 20° in azimuth. With this arrangement (where both photons of the π^0 decay were also identified) we took data which were statistically significant up to 6.5 GeV/c in p_T . For higher values of p_T , the large solid angle (3 sr total fiducial area) of our "normal geometry" was required. This consisted of four calorimeters, placed at a distance of 0.86 m from the interaction region. In this configuration $\geq 90\%$ of all $\pi^0 \rightarrow 2\gamma$ events above $p_T = 8$ GeV/c appeared as single, merged, unresolved, electromagnetic showers. The opening angle in the η decay is larger and we were able to resolve the two photons from the η decay throughout the p_T range, in both configurations.

The trigger used for the experiment is a requirement of sufficient energy deposit in the calorimeter, and is described in detail elsewhere [2,3].

The retracted geometry data presented here are based on an integrated luminosity of 0.65×10^{36} cm⁻² at $\sqrt{s} = 30.6$ GeV, 1×10^{36} at $\sqrt{s} = 52.7$ GeV, and 0.98×10^{36} at $\sqrt{s} = 62.4$ GeV. The normal geometry data were mostly taken at $\sqrt{s} = 62.4$ GeV and represent an integrated luminosity of 3.62×10^{37} cm⁻².

DATA ANALYSIS

The selection of each candidate was done by requiring at least two reconstructed photon showers; the asymmetry of the photon pair, $\alpha = |E_1 - E_2|/E_{\text{tot}}$, was restricted to values smaller than 0.4, our detection efficiency being constant over this range of α .

The data from both geometrical arrangements covered a p_T range of 3 to 11 GeV/c. The lower limit was imposed by the trigger thresholds and the upper limit by the available statistics. Figures 2a and b show mass spectra for the two different geometrical arrangements. The backgrounds under the peaks do not account for more than 50% and are of two kinds. One is due to the pairing of uncorrelated showers. The other kind of background, which is mainly near the π^0 peak, comes from beam-gas interactions leading to false shower signals. This was removed by imposing further restrictions on energy deposition and on the radius of the electromagnetic showers in the calorimeter. These requirements were found effective in eliminating false showers and rejected only 5% of the signal.

For each p_T interval the shape of the η -mass spectrum was parametrized as a Gaussian on top of a quadratic background; by minimizing χ^2 , the amounts of signal and background, the centroid and width of the Gaussian, and the background shape parameters were determined. The widths are consistent with the calorimeter energy resolution. Calculating the acceptance of the apparatus for each p_T interval using a Monte Carlo technique and correcting for the $\eta \rightarrow 2\gamma$ branching ratio, the η production cross-section shown in the table was obtained. The observed η/π^0 ratio of events -- after background subtraction -- was corrected by the relative η/π^0 geometrical and trigger acceptances. Therefore the η/π^0 cross-section ratio was free of most systematic biases such as normalization uncertainties, etc.

Any directly produced photons [4-7] are included in the π^0 sample for the normal geometry. The existence of such photons would lower the ratio η/π^0 only for this geometry (i.e. $p_T > 7$ GeV/c) while it would have no effect for the retracted geometry ($p_T < 7$ GeV/c).

RESULTS AND DISCUSSION

The η/π^0 inclusive cross-section ratio as a function of p_T is shown in Fig. 3, for the retracted geometry, for the three different values of \sqrt{s} . An average value of $\eta/\pi^0 = 0.57 \pm 0.08$ describes the data well for the range of p_T of this geometry ($3 < p_T < 7$ GeV/c) and $31 < \sqrt{s} < 62$ GeV. The above value is consistent with previous measurements at the ISR [8], while it is higher than the results at FNAL energies [9,10] taken at lower values of \sqrt{s} and of p_T . Figure 4 shows the η/π^0 cross-section ratio for $\sqrt{s} = 62.4$ GeV and for both retracted and normal geometries, as a function of p_T , for p_T 's up to 11 GeV/c. For $p_T > 7$ GeV/c, the η/π^0 ratio is consistent with an average value of 0.53 ± 0.07 (the errors quoted on these average values include an estimate of the systematic errors).

Some theoretical calculations [4-7] suggest that there is a sizeable single-photon production at high p_T . Assuming that a possible drop in the average value of the η/π^0 cross-section ratio in going from the retracted to the normal geometry is due exclusively to this effect, then the average γ/π^0 cross-section ratio, for p_T between 7 and 11 GeV/c, would be $\gamma/\pi^0 = 0.08 \pm 0.18$.

REFERENCES

- [1] J. Cobb et al., Nucl. Instrum. Methods 140 (1976) 1977;
J. Cobb et al., Nucl. Instrum. Methods 158 (1979) 93.
- [2] C. Kourkouvelis et al., Inclusive π^0 production at very large p_T at the ISR, preceding Letter.
- [3] C. Kourkouvelis et al., Study of resolved high p_T neutral pions at the CERN ISR, Phys. Lett. B (in press).
- [4] G. Farrar and S.C. Frautschi, Phys. Rev. Lett. 36 (1976) 1017.
- [5] F. Halzen and D.M. Scott, Phys. Rev. Lett. 40 (1978) 1117 and University of Wisconsin preprint COO-881-21 (1978).
- [6] R. Rückl, S.J. Brodsky and J.F. Gunion, SLAC-PUB-2115 (1978).
- [7] A.P. Contogouris, S. Papadopoulos and M. Hongah, Scale violation effects in large p_T direct photon production, Phys. Rev. D1 (in press).
- [8] F.W. Büsler et al., Phys. Lett. 55B (1975) 232.
- [9] G. Donaldson et al., Phys. Rev. Lett. 40 (1978) 684.
- [10] B. Cox, Fermilab Experiment 95, results presented at the Lepton and Photon Conference, Hamburg, August 1977.

Invariant cross-sections for the reaction $pp \rightarrow \eta X$

p_T range (GeV/c)	$\langle p_T \rangle$ (GeV/c)	$Ed^3\sigma/dp^3$ ($\text{cm}^2 \text{ c}^3/\text{GeV}^2$)
$\sqrt{s} = 30.6 \text{ GeV}$		
3.1-3.5	3.30	$(1.29 \pm 0.21) \times 10^{-32}$
3.5-4.0	3.75	$(2.77 \pm 0.58) \times 10^{-33}$
$\sqrt{s} = 52.7 \text{ GeV}$		
3.1-3.5	3.30	$(6.38 \pm 0.75) \times 10^{-32}$
3.5-4.0	3.75	$(1.82 \pm 0.22) \times 10^{-32}$
4.0-5.0	4.50	$(2.77 \pm 0.48) \times 10^{-33}$
5.0-6.0	5.50	$(2.30 \pm 0.49) \times 10^{-34}$
$\sqrt{s} = 62.4 \text{ GeV}$		
3.1- 3.5	3.30	$(7.65 \pm 0.94) \times 10^{-32}$
3.5- 4.0	3.75	$(2.12 \pm 0.26) \times 10^{-32}$
4.0- 5.0	4.50	$(3.79 \pm 0.48) \times 10^{-33}$
5.0- 7.0	6.00	$(1.63 \pm 0.28) \times 10^{-34}$
7.0- 8.0	7.50	$(1.51 \pm 0.21) \times 10^{-35}$
8.0- 9.0	8.50	$(4.54 \pm 0.73) \times 10^{-36}$
9.0-10.0	9.50	$(1.18 \pm 0.29) \times 10^{-36}$
10.0-11.0	10.50	$(3.51 \pm 1.43) \times 10^{-37}$

Figure captions

- Fig. 1 : Apparatus arrangement for a) "retracted" and b) "normal" geometry.
- Fig. 2 : Digamma invariant mass spectrum for a) "retracted" and b) "normal" geometry.
- Fig. 3 : η/π^0 cross-section ratio from "retracted" geometry for three different values \sqrt{s} .
- Fig. 4 : η/π^0 cross-section ratio for all data combined as a function of p_T , at $\sqrt{s} = 62.4$ GeV, using "retracted" geometry, $\pi^0 \rightarrow \gamma\gamma$ data, up to 7 GeV/c, and unresolved ($\pi^0 + \gamma$) cross-sections from the "normal" geometry above 7 GeV/c.

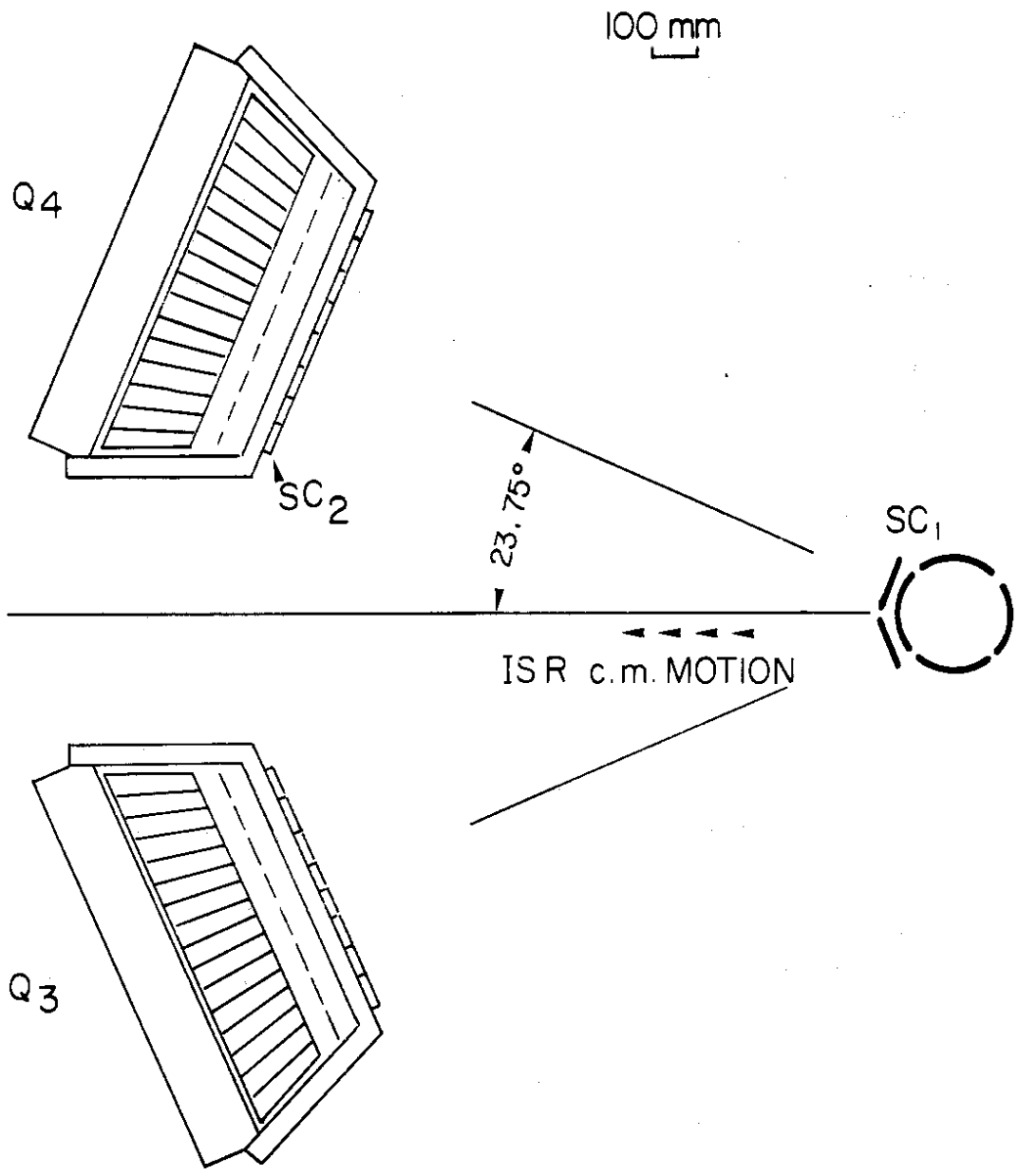


Fig. 1a

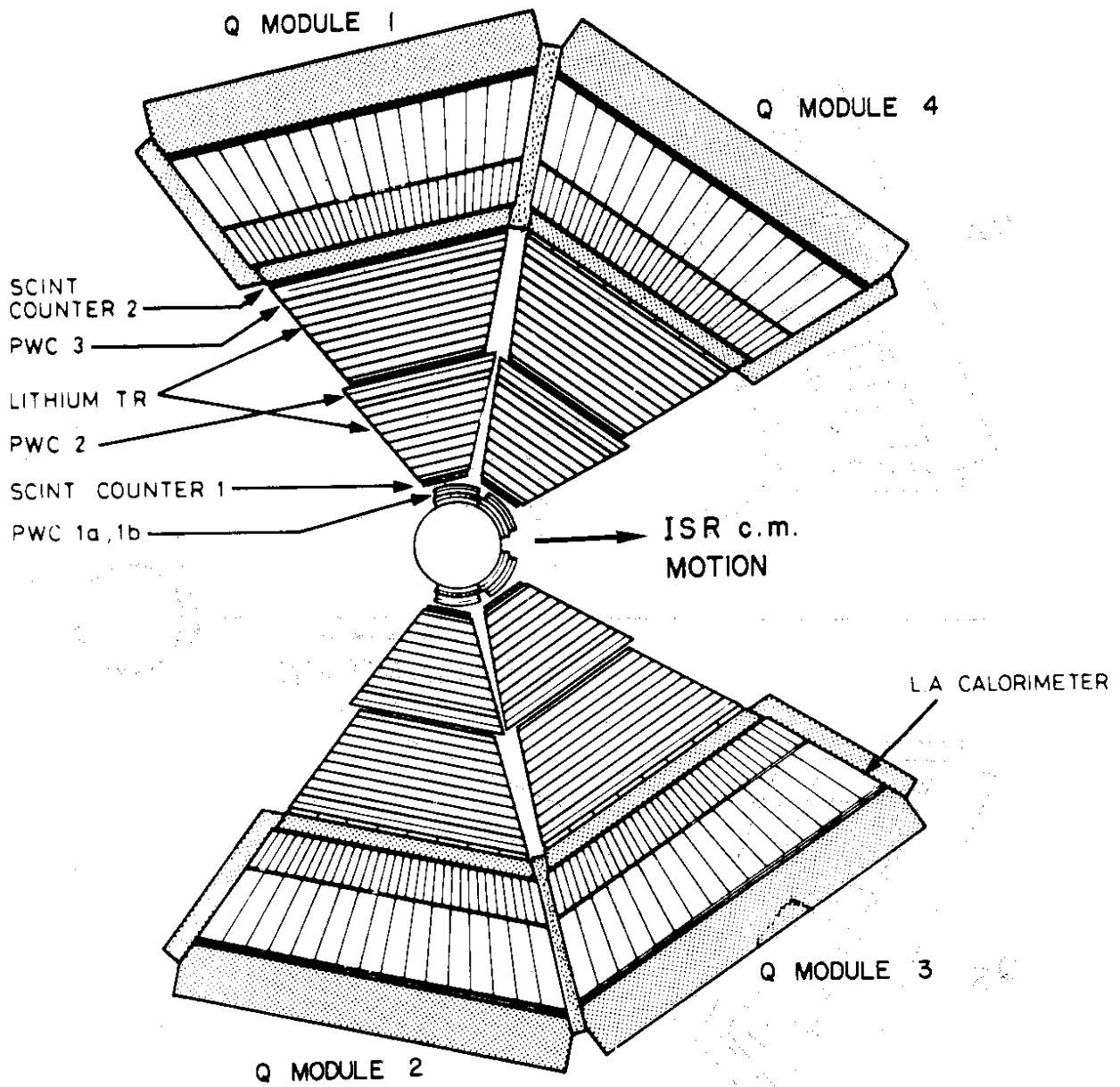


Fig. 1b

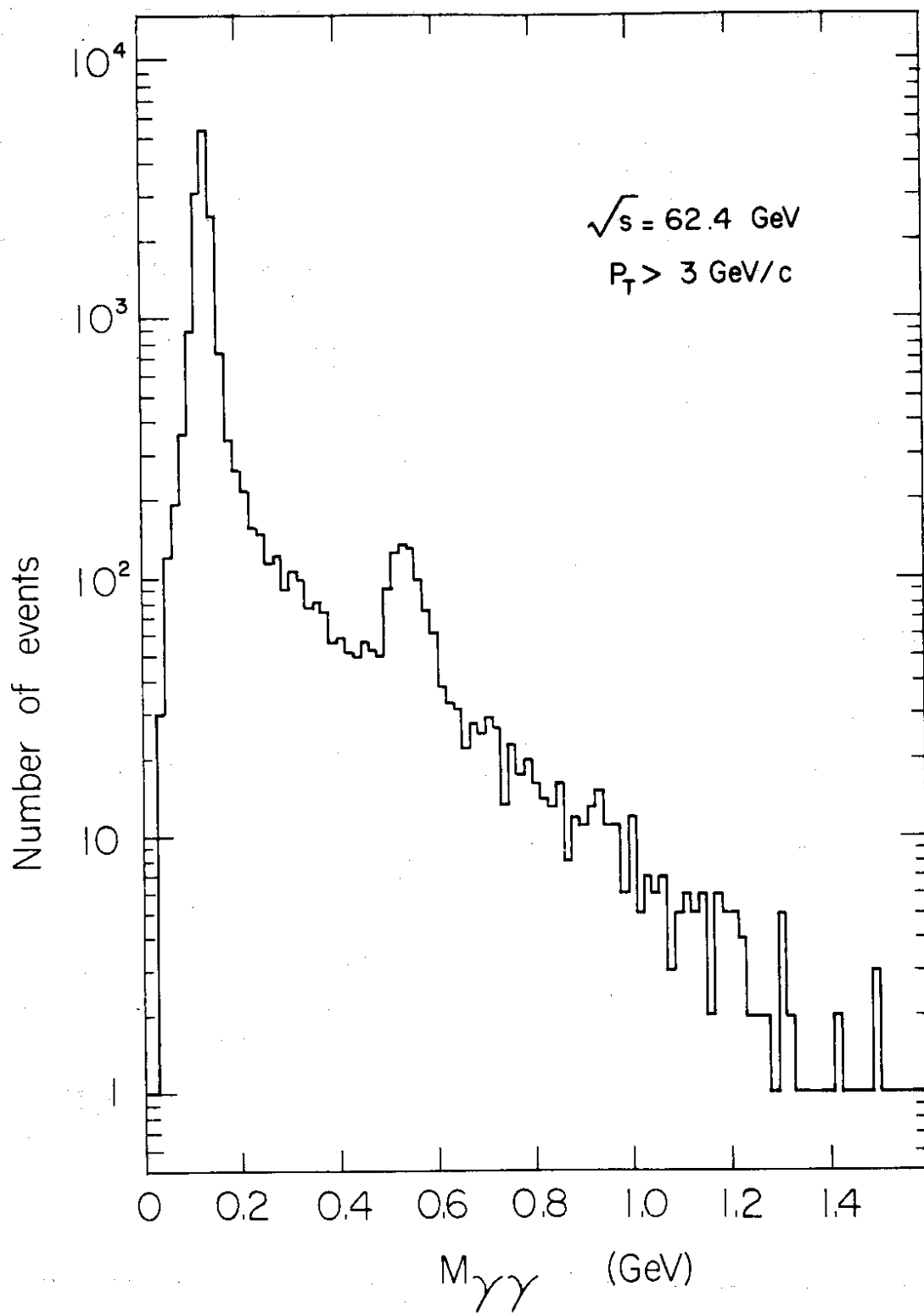


Fig. 2a

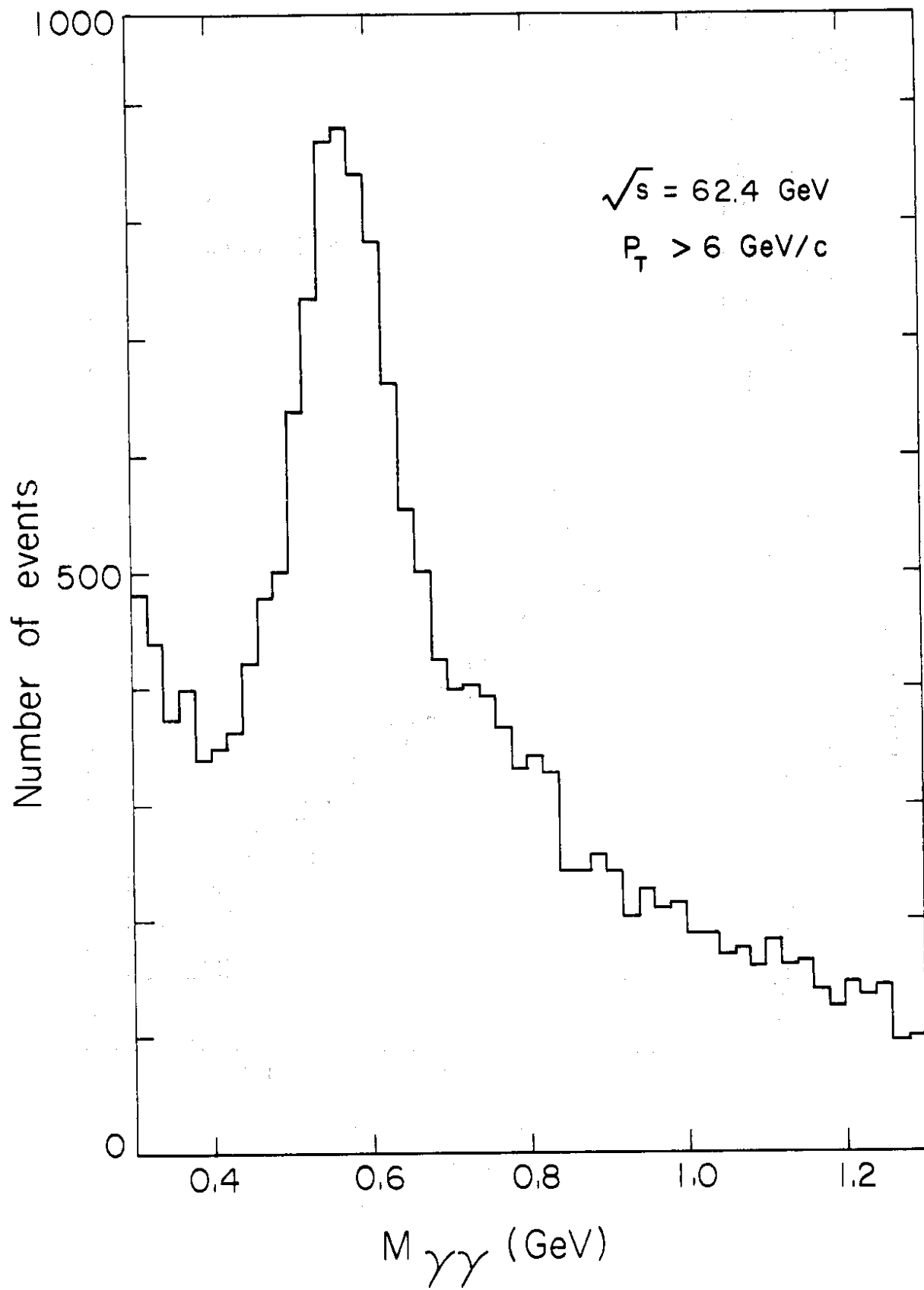


Fig. 2b

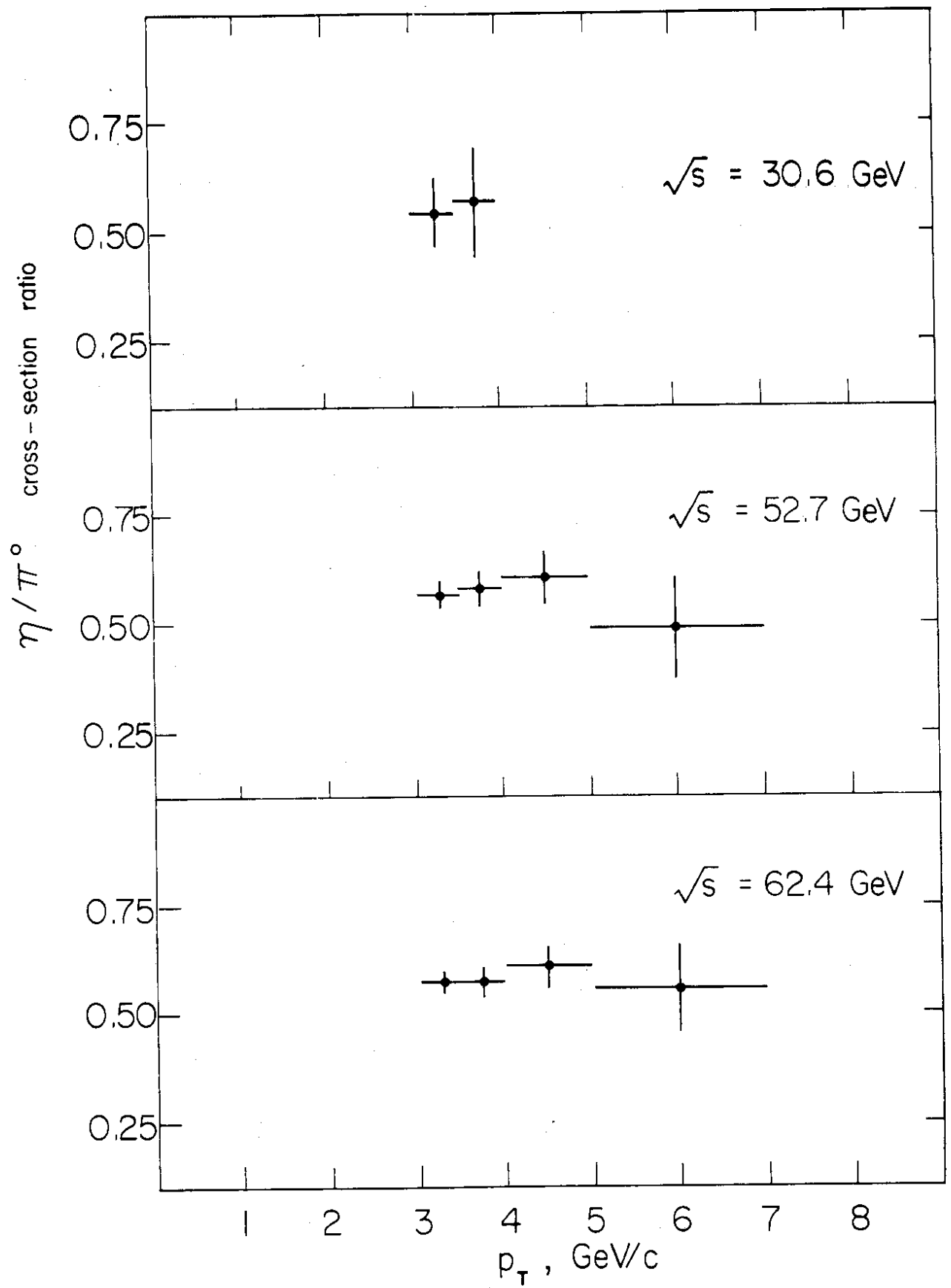


Fig. 3

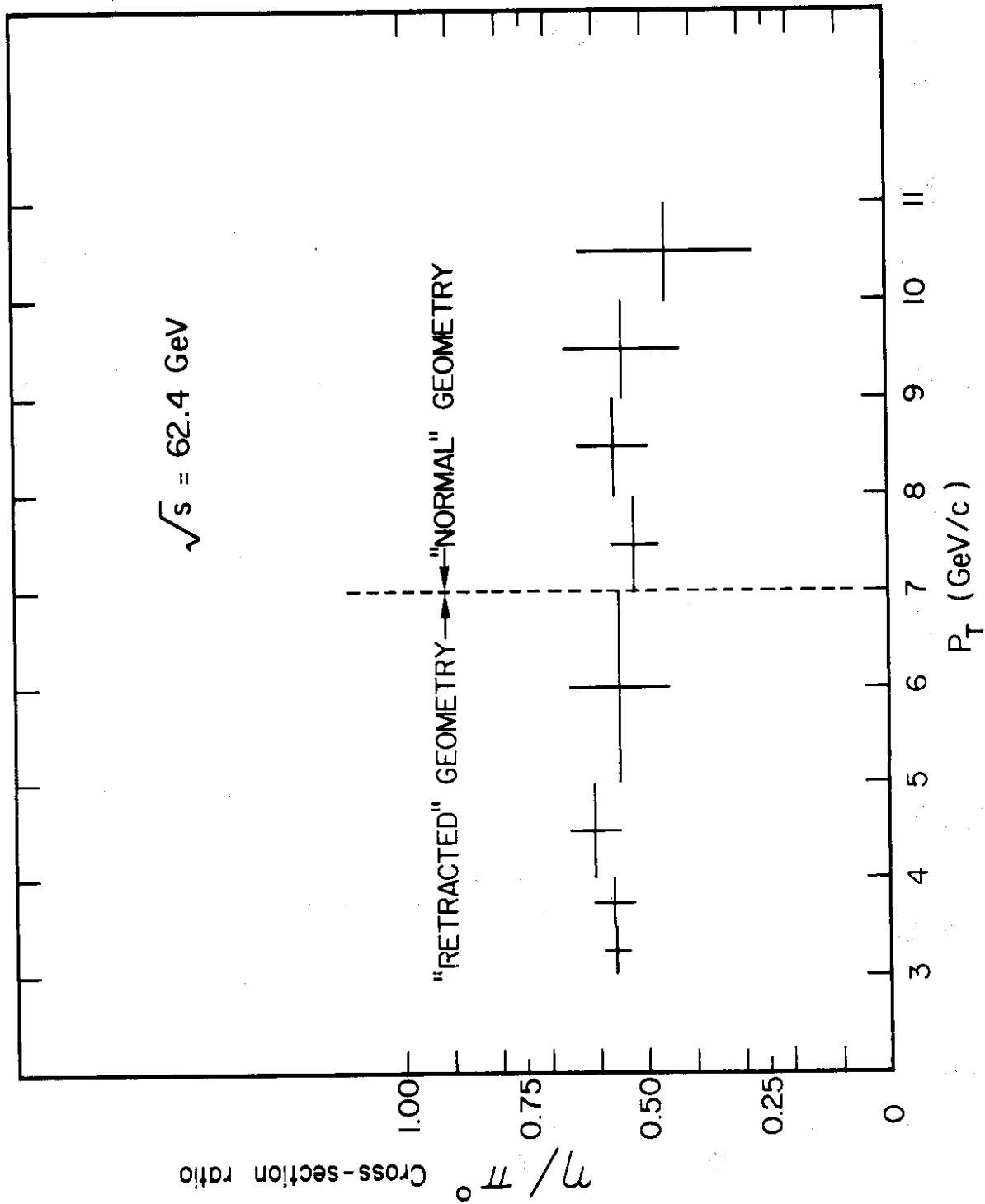


Fig. 4

23